



## Elastic rotation of *Escherichia coli* F<sub>0</sub>F<sub>1</sub> having $\epsilon$ subunit fused with cytochrome *b*<sub>562</sub> or flavodoxin reductase



Hideyuki Oka<sup>a</sup>, Hiroyuki Hosokawa<sup>b</sup>, Mayumi Nakanishi-Matsui<sup>b</sup>, Stanley D. Dunn<sup>c</sup>, Masamitsu Futai<sup>b</sup>, Atsuko Iwamoto-Kihara<sup>a,\*</sup>

<sup>a</sup> Department of Bioscience, Nagahama Institute of Bioscience and Technology, Nagahama, Shiga 526-0829, Japan

<sup>b</sup> Department of Biochemistry, Faculty of Pharmaceutical Sciences, Iwate Medical University, Yahaba, Iwate 028-3694, Japan

<sup>c</sup> Department of Biochemistry, University of Western Ontario, London, Ontario N6A 5C1, Canada

### ARTICLE INFO

#### Article history:

Received 25 February 2014

Available online 13 March 2014

#### Keywords:

ATP synthase

F<sub>0</sub>F<sub>1</sub>

Molecular motor

Elastic rotation

$\epsilon$  Subunit

Energy coupling

### ABSTRACT

Intra-molecular rotation of F<sub>0</sub>F<sub>1</sub> ATP synthase enables cooperative synthesis and hydrolysis of ATP. In this study, using a small gold bead probe, we observed fast rotation close to the real rate that would be exhibited without probes. Using this experimental system, we tested the rotation of F<sub>0</sub>F<sub>1</sub> with the  $\epsilon$  subunit connected to a globular protein [cytochrome *b*<sub>562</sub> ( $\epsilon$ -Cyt) or flavodoxin reductase ( $\epsilon$ -FlavR)], which is apparently larger than the space between the central and the peripheral stalks. The enzymes containing  $\epsilon$ -Cyt and  $\epsilon$ -FlavR showed continual rotations with average rates of 185 and 148 rps, respectively, similar to the wild type (172 rps). However, the enzymes with  $\epsilon$ -Cyt or  $\epsilon$ -FlavR showed a reduced proton transport. These results indicate that the intra-molecular rotation is elastic but proton transport requires more strict subunit/subunit interaction.

© 2014 Elsevier Inc. All rights reserved.

### 1. Introduction

ATP synthase (F<sub>0</sub>F<sub>1</sub>), ubiquitously found in membranes of bacteria, mitochondria, and chloroplast thylakoids, synthesizes ATP coupled with an electrochemical proton gradient generated by the electron transport chain [1–3]. Bacteria have the simplest version consisting of a peripheral sector F<sub>1</sub> ( $\alpha_3\beta_3\gamma\delta\epsilon$ ) with three catalytic  $\beta$  subunits, and a membrane integral F<sub>0</sub> (*ab*<sub>2</sub>*c*<sub>10–15</sub>) with the proton pathway formed from the *a* subunit and the multiple *c* subunits (*c*-ring).

Catalysis and transport are coupled through the intra-molecular rotations, consistent with the “binding change mechanism” [1]. The *c*-ring rotation powered by H<sup>+</sup> transport through two aqueous half-channels and multiple Asp/Glu residues of the *c*-ring supports the sequential conformational changes of catalytic site in each of the three  $\beta$  to synthesize ATP [1–3].

Single molecule observations of *Escherichia coli* F<sub>0</sub>F<sub>1</sub> indicated clearly that the  $\gamma\epsilon c_{10}$  complex rotates against the  $\alpha_3\beta_3\delta ab_2$  subunits during ATP hydrolysis [4–7]. Experimentally, the F<sub>0</sub>F<sub>1</sub> was immobilized on the glass surface through the  $\alpha$  or  $\beta$  subunit and an actin filament probe attached to the *c* subunit showed counterclockwise rotation [4,6] (Fig. 1A). The probe attached to the  $\beta$ ,  $\alpha$ , or *a* subunit also indicated the rotation of  $\alpha_3\beta_3\delta ab_2$  complex against  $\gamma\epsilon c_{10}$ , when the purified or membrane bound enzyme was immobilized through the *c*-ring [6,7] (Fig. 1B). However, the rotation rates observed were slow due to the large viscous drag on the actin filament. Experiments using single molecule FRET analysis also showed the rotation of membrane-bound F<sub>0</sub>F<sub>1</sub> during ATP synthesis/hydrolysis [8].

Although the detailed tertiary structure of F<sub>0</sub>F<sub>1</sub> is still unknown, the structure of mammalian F<sub>1</sub> with its *c*-ring has been reported [9]. The higher-ordered structure obtained by electron microscopy [10] clearly showed the central and peripheral stalks connecting F<sub>1</sub> and F<sub>0</sub>, corresponding to the rotor and the stator assembly, respectively. The central stalk was a part of the rotor  $\gamma\epsilon c_{10}$ , formed from the  $\gamma$  and the  $\epsilon$  subunits and loop regions of the *c* subunits, whereas peripheral stalk was formed from the subunits *b* and  $\delta$ . The microscopic structure also indicated the presence of an open space between the two stalks [10].

Detailed structures of the  $\epsilon$  subunit forming the central stalk were extensively studied. The isolated  $\epsilon$  subunit showed two

Abbreviations: C<sub>12</sub>E<sub>8</sub>, octaethylene glycol monododecyl ether; MES, 2-(*N*-morpholino)ethanesulfonic acid; MOPS, 3-(*N*-morpholino)propanesulfonic acid; Tricine, *N*-(2-hydroxy-1,1-bis(hydroxymethyl)ethyl)glycine; Tris, tris(hydroxymethyl)aminomethane;  $\epsilon$ -Cyt,  $\epsilon$  subunit connected with cytochrome *b*<sub>562</sub>;  $\epsilon$ -FlavR,  $\epsilon$  subunit connected with flavodoxin reductase.

\* Corresponding author. Fax: +81 749 64 8140.

E-mail address: [a.iwamoto@nagahama-i-bio.ac.jp](mailto:a.iwamoto@nagahama-i-bio.ac.jp) (A. Iwamoto-Kihara).

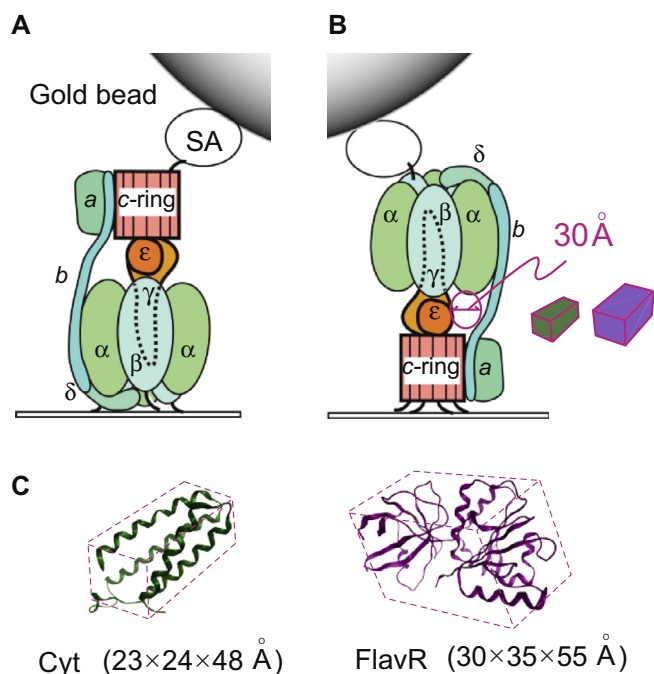


**Fig. 1.** Rotation observations of the F<sub>0</sub>F<sub>1</sub> using 60 nm bead probes. (A) Rotation observation using the gold bead attached to the c-ring of F<sub>0</sub>F<sub>1</sub>. The F<sub>0</sub>F<sub>1</sub> was immobilized on the Ni-coated glass via the histidine-tag at the amino termini of the β subunits. The biotinylated gold bead was linked to the c subunit through the streptavidin (SA). Upon ATP hydrolysis, the bead revolution was observed. (B) Rotation observation using the gold bead attached to the β subunit of F<sub>0</sub>F<sub>1</sub>. The F<sub>0</sub>F<sub>1</sub> was immobilized through the c-ring, and the gold bead attached to the β subunit. The space between the central and the peripheral stalks was estimated [10], and indicated as a sphere space (diameter, ~30 Å). The green and purple cuboids were shown as the fused proteins cytochrome b<sub>562</sub> and flavodoxin reductase, respectively. (C) Ribbon models of proteins that fused to the carboxyl termini of the ε subunits. Cytochrome b<sub>562</sub> (23 × 24 × 48 Å) (Cyt, PDB ID: 256B) [27] and Flavodoxin reductase (30 × 35 × 55 Å) (FlavR, PDB ID: 1FDR) [28] are shown.

carboxyl-terminal helices folded near the amino terminal β-sandwich domain [11,12]. However, according to the recent crystal structure of F<sub>1</sub> [13], two ε subunit helices were extended along the coiled-coil of the γ subunit, and the second helix was penetrated between the rotor and the stator to prevent the γ subunit rotation. This structure seemed consistent with the inhibition of F<sub>1</sub> ATPase with the ε subunit [14]. Crosslink studies suggested that the ε subunit adopted both folded and extended conformations in the F<sub>0</sub>F<sub>1</sub> [15,16].

Considering the function and structure of the central stalk, it was of interest to study the F<sub>0</sub>F<sub>1</sub> carrying the ε subunits fused to globular proteins at the carboxyl terminus [17]. The fused proteins such as cytochrome b<sub>562</sub>, flavodoxin, and flavodoxin reductase were large enough to affect the enzyme catalysis (Fig. 1C). As expected, the extra moieties caused significantly reduced ATP-driven proton transport while ATPase activities were retained [17]. The wild-type ε subunit inhibited rotation and ATPase activity of F<sub>1</sub> sector, whereas the ε-Cyt (ε subunit connected with cytochrome b<sub>562</sub>) showed no effect [18], indicating that ε-Cyt lost normal interaction of its carboxyl-terminal region with other subunits. Thus, we concluded that the globular proteins fused to the ε subunits affected rotation, leading to lower proton transport. However, no studies were carried out to address the effect of ε-Cyt on rotational catalysis of F<sub>0</sub>F<sub>1</sub>.

In this study, we observed faster rotation of the F<sub>0</sub>F<sub>1</sub> with a gold bead probe (60 nm) attached to the β subunit or the c-ring (Fig. 1A, B). Since viscous drag on the revolving small bead was substantially low, rotation rates observed were 30–50-fold higher than

that with actin probe, and close to the rate which would be exhibited without a probe. This experimental system prompted us to test the rotation of F<sub>0</sub>F<sub>1</sub> with the ε subunit connected to the extra globular proteins because they reduced energy coupling to H<sup>+</sup>-pumping. Surprisingly, the beads attached to the β subunit of the enzymes containing the ε-Cyt and the ε-FlavR showed rates similar to that of the wild-type enzyme. Considering the dimensions of the extra domains included into the γεc<sub>10</sub> complex, these studies suggested that the F<sub>0</sub>F<sub>1</sub> has elasticity which permits rotation of the large central stalk.

## 2. Materials and methods

### 2.1. Recombinant plasmids

F<sub>0</sub>F<sub>1</sub> operon containing the genes for histidine-tagged β subunit and the c subunit with cGlu2Cys substitution was previously described [6]. Genes for the ε-fusions were introduced into pBUR13DX, a derivative of pBWU13 [4], carrying all F<sub>0</sub>F<sub>1</sub> subunit genes with the sequences for the biotin- and the histidine-tags at the amino termini of the β and the c subunit genes, respectively [19]. Using *Sac*I site in the β subunit gene and newly introduced *Xba*I site 323 bp downstream of the termination codon of the ε subunit gene, the sequences for the ε-Cyt and the ε-FlavR (formerly named as ε-Red and ε-Yellow, respectively) [17] were introduced. Genes for the ε-fusions with a linker sequence between the ε and the fusion proteins (ε-L-Cyt and ε-L-FlavR) [17] were also introduced.

### 2.2. Preparation of F<sub>0</sub>F<sub>1</sub>

Recombinant plasmids were introduced into the *E. coli* strain DK8 (*Δ*atpB-C) [20]. Membrane vesicles (containing about 40 mg of proteins) prepared after disruption of the cells grown on glycerol were suspended in 3.2 ml of Buffer A [40 mM MES-Tricine (pH7.0 at 25 °C), 10 mM MgCl<sub>2</sub> and 20%(w/v) glycerol] then solubilized by addition of 0.8 ml of 10%(w/v) C<sub>12</sub>E<sub>8</sub> (final concentration of 2%). The suspension was centrifuged at 125,000×g for 60 min, and the supernatant was slowly applied to the Ni-nitrilotriacetic acid agarose column (0.6 × 1.5 cm, Qiagen) equilibrated with Buffer B [20 mM MES-Tricine (pH7.0 at 25 °C), 5 mM MgCl<sub>2</sub>, 10% glycerol and 2% C<sub>12</sub>E<sub>8</sub>]. The column was washed with 6 ml of Buffer C [20 mM MES-Tricine (pH7.0 at 25 °C), 5 mM MgCl<sub>2</sub>, 10% glycerol, 0.1% C<sub>12</sub>E<sub>8</sub>, 0.03% (w/v) L-α-phosphatidylcholine and 20 mM imidazole]. F<sub>0</sub>F<sub>1</sub> was eluted with the same buffer by increasing the imidazole concentration up to 200 mM dialyzed against Buffer C containing 25% glycerol. All procedures described above were carried out at 4 °C. Purified enzyme was quickly frozen in liquid nitrogen and stored at –80 °C until use.

### 2.3. DCCD sensitivities of membrane and F<sub>0</sub>F<sub>1</sub> ATPase activities

Membranes (20 μg protein) or purified F<sub>0</sub>F<sub>1</sub> (4 μg of protein) were treated in 100 μl of 50 mM Tris–HCl (pH8.0) buffer containing 40 μM DCCD (*N,N*-dicyclohexylcarbodiimide), 2 mM MgCl<sub>2</sub>, 300 mM KCl for 15 min at 22 °C. ATPase activity of 50 μl aliquot was assayed at 22 °C with coupled NADH oxidation in the presence of ATP regeneration system [21].

### 2.4. Rotation observation of immobilized enzymes

Rotations of both F<sub>0</sub>F<sub>1</sub> molecules immobilized through the β subunits and the c-ring were observed using essentially the same procedures for F<sub>1</sub> rotations as described previously [18]. Briefly, a flow cell was filled with Buffer D [10 mM MOPS-KOH, 50 mM

KCl, 2 mM MgCl<sub>2</sub>, 0.1% C<sub>12</sub>E<sub>8</sub>, 0.03% L- $\alpha$ -phosphatidylcholine, pH7.0] containing 40–50 nM F<sub>0</sub>F<sub>1</sub>, and incubated for 10 min at 24 °C. After washing the flow cell, the same buffer containing 10 mg/ml bovine serum albumin (BSA), streptavidin and biotinylated gold beads were applied. Immediately after addition of the Buffer D with 2 mM ATP and ATP regeneration system but without detergent and phospholipids, images of the gold beads illuminated by laser light were followed under a dark field microscope (BX51WI-CDEVA-F, Olympus) and captured with an ICCD camera (Photron Co.) at 2000 fps (frames per second). Mostly, the observations were finished within 20 min after ATP addition. The data was analyzed using Image J (National Institutes of Health) [22] and 'DoAll' kindly supplied by Dr. Bradley Steel, University of Oxford. Rotation rate of F<sub>0</sub>F<sub>1</sub> was estimated as reciprocal for geometric mean of the times that required for every 360-degree revolution of the probe [21].

### 2.5. Other procedures

Western blot analysis was carried out using anti-*E. coli*  $\epsilon$  antibodies [23]. Protein concentrations were determined by the methods of Lowry *et al.* (for membranes) and Bradford (for F<sub>0</sub>F<sub>1</sub>) using bovine serum albumin as a standard [24,25].

## 3. Results and discussion

### 3.1. Rotations of F<sub>0</sub>F<sub>1</sub> immobilized through the $\beta$ subunits and the $c$ -ring

Previously, single molecule observations indicated clearly that the  $\gamma\epsilon c_{10}$  complex rotated against the  $\alpha_3\beta_3\delta ab_2$  subunits during ATP hydrolysis [4–7]. However, the rotation rates observed were much slower than those expected from ATPase activity due to the large viscous drag on rotating actin probe. We tested ATP-dependent revolutions of gold beads (60–100 nm diameter) and a 100 nm bead-dimer attached to the  $c$ -ring to estimate F<sub>0</sub>F<sub>1</sub> rotation (Fig. 1A). Time courses with 60 nm bead (Fig. 2A) clearly indicated 30–50-fold faster rotation (217 rps) (Table 1) than that of the actin filament probes (Fig. 2B, triangles). The 60, 80 and 100 nm beads showed essentially the same revolving speed,

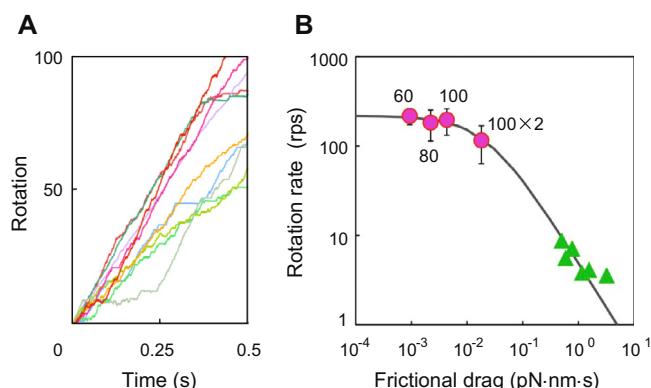


**Fig. 2.** Rotation rates estimated with the probes attached to the F<sub>0</sub>F<sub>1</sub>  $c$  subunit. (A) Time courses of the 60 nm gold bead revolutions attached to the  $c$ -ring. (B) Rotation rates with various probes attached to the  $c$ -ring. Rotation rates were estimated using 60, 80 and 100 nm beads and double beads (100-nm  $\times$  2) attached to the  $c$ -ring. Approximated curve of rotation rates is shown by the formula below; Rotation rate (rps) =  $1/(1/V_{no-load} + 2\pi\xi/N)$  here,  $V_{no-load}$  is rotation rate without probes;  $\xi$  is frictional drag of the probe;  $N$  is rotational torque generated with F<sub>0</sub>F<sub>1</sub> [6,19]. Rates by using of small beads (pink circle) are shown together with those of actin filaments previously reported (green triangle) [4,6]. (For interpretation of the references to colour in this figure legend, the reader is referred to the web version of this article.)

**Table 1**

Comparison of the rotation rates between F<sub>0</sub>F<sub>1</sub> and F<sub>1</sub>.

Molecule	Subunit probe attached	Rotation (rps)
F <sub>0</sub> F <sub>1</sub>	$c$	217
F <sub>0</sub> F <sub>1</sub>	$\beta$	172
F <sub>1</sub>	$\gamma$	381
F <sub>1</sub> (+ $\epsilon$ )	$\gamma$	197

The molecules used were immobilized through the histidine-tags in the  $c$  or the  $\beta$  subunit. Average rotation rates were estimated by 60 nm beads that attached to the indicated subunits. The rotation rates of the  $\gamma$  subunit in F<sub>1</sub> with (+  $\epsilon$ ) or without the  $\epsilon$  subunit were cited from reference [18] and unpublished result (M. Nakanishi-Matsui), respectively.

indicating that their rates were close to the  $\gamma\epsilon c_{10}$  rotation that would be expected without viscous drag (Fig. 2B). The rate with the 100 nm bead-dimer was significantly slower ( $\sim$ 120 rps). The bead attached to the  $\beta$  subunit of F<sub>0</sub>F<sub>1</sub> (Fig. 1B) showed slightly slower but similar rotation rate as that attached to the  $c$ -ring (Table 1), confirming that the actin probe used in two different modes gave essentially the same speed [6].

It was noteworthy that the rotation rates ( $\sim$ 200 rps) of F<sub>0</sub>F<sub>1</sub> were consistent with that of the F<sub>1</sub> with  $\epsilon$  [18] which was about 1/2 of the rate of F<sub>1</sub> without  $\epsilon$  subunit ( $\sim$ 400 rps) (Table 1). The rotation of F<sub>0</sub>F<sub>1</sub> frequently paused for several tens of milliseconds (Fig. 2A), similar to the observation of the F<sub>1</sub>  $\gamma$  rotation with  $\epsilon$  subunit [18]. Since increasing pauses in the presence of the  $\epsilon$  subunit reduced the F<sub>1</sub> rotation rate, the F<sub>0</sub>F<sub>1</sub> having endogenous  $\epsilon$  was suggested to rotate with pausing as an intrinsic property.

### 3.2. Properties of the strains carrying $\epsilon$ -Cyt and $\epsilon$ -FlavR in the histidine- and biotin-tagged F<sub>0</sub>F<sub>1</sub>

Since the rotation rate of F<sub>0</sub>F<sub>1</sub> determined using the 60 nm bead was close to what would be expected without the probe, this system could be used to analyze the rotations of the mutant enzymes, especially those with altered interaction between F<sub>1</sub> and F<sub>0</sub>. We addressed the rotational properties of the enzymes carrying  $\epsilon$ -Cyt and  $\epsilon$ -FlavR, which may provide evidence of the roles of the central stalk during rotation.

We constructed strains harboring the recombinant plasmids coding for entire F<sub>0</sub>F<sub>1</sub> genes with the  $\epsilon$ -Cyt and the  $\epsilon$ -FlavR. As shown previously [17], the strain with the  $\epsilon$ -Cyt could grow by oxidative phosphorylation essentially the same as the wild type, whereas the strain with the  $\epsilon$ -FlavR could not, suggesting that the F<sub>0</sub>F<sub>1</sub> with  $\epsilon$ -FlavR was defective in ATP synthesis, but that enzyme with  $\epsilon$ -Cyt may be similar to wild type. The membrane fractions from strains carrying both of the  $\epsilon$ -fusion genes contained similar amounts of  $\epsilon$  subunit as the wild type (data not shown).

**Table 2**

ATPase activities and rotation rates of the F<sub>0</sub>F<sub>1</sub> having wild-type  $\epsilon$ ,  $\epsilon$ -Cyt and  $\epsilon$ -FlavR subunits.

$\epsilon$ subunits	ATPase activity ( $\mu$ moles/mg·min)	Molecular observation Single rotation time (ms)	Rotation rate (rps)
Wild type	6.9	5.82	172*
$\epsilon$ -Cyt	7.2	5.41	185
$\epsilon$ -FlavR	3.2	6.77	148

The F<sub>0</sub>F<sub>1</sub> holoenzymes containing wild-type  $\epsilon$ ,  $\epsilon$ -Cyt and  $\epsilon$ -FlavR were ATPase assayed at 25 °C. The revolutions of 60 nm beads attached to the  $\beta$  subunit of immobilized F<sub>0</sub>F<sub>1</sub> were observed. Geometric means of the time required for a single rotation were estimated, and the rotation rates were also determined (\*cited from Table 1).

The membranes prepared from the cells having the  $\epsilon$ -Cyt showed 1.5-fold higher ATPase activity than those from the wild type, although ATP-driven proton transport was reduced to about 69% (Table S1). Membranes having the larger fusion protein,  $\epsilon$ -FlavR, also reduced  $H^+$ -pumping to about 26% of that of the wild type although their ATPase activities were similar (Table S1). The membrane ATPase activities with the wild-type  $\epsilon$ ,  $\epsilon$ -Cyt, and  $\epsilon$ -FlavR were reduced by DCCD treatment by 71%, 59% and 40%, respectively (Table S1). These results were consistent with those previously reported for the enzymes not engineered for rotation observation [17], confirming that the globular proteins fused with the  $\epsilon$  subunit affected energy coupling between ATP synthesis/hydrolysis and  $H^+$ -translocation.

### 3.3. Purification of holoenzymes containing the $\epsilon$ with fusion proteins

The  $F_0F_1$  holoenzymes having  $\epsilon$ -Cyt and  $\epsilon$ -FlavR were solubilized from the membranes, and purified with the Ni-NTA-agarose column. All enzymes showed essentially the same subunit composition except that the  $\epsilon$  subunits with fusion proteins showed increased molecular weight (Fig. S1A, arrow heads). No degradation of  $\epsilon$ -Cyt or  $\epsilon$ -FlavR was detectable with anti- $\epsilon$  antibodies (Fig. S1B), with or without the linker between  $\epsilon$  and fused protein. The  $c$  subunits were hardly visible in these preparations since amount of  $F_0F_1$  was too low to detect all subunits. The presence of the  $c$  subunit was supported by purification procedure used, and confirmed by immobilization to Ni-coated glass similar to the wild-type enzyme. The specific activity of each enzyme was observed at 25 °C (Table 2).

### 3.4. Elastic rotation of the $F_0F_1$ molecules

It became of interest to know whether the  $F_0F_1$ 's with fused globular proteins could rotate similar to the wild type because they had high ATPase activities, or if they rotated slower than the wild type because their energy coupling to proton transport was low. For observing rotation, the  $F_0F_1$  with the  $\epsilon$ -Cyt or the  $\epsilon$ -FlavR was immobilized on the glass surface through the  $c$  subunits, and the 60 nm bead was attached to the  $\beta$  subunit (Fig. 1B).

Upon ATP addition, the  $F_0F_1$  with  $\epsilon$ -Cyt and  $\epsilon$ -FlavR rotated following the similar time courses to the wild type (Fig. 3A–C). We analyzed the single rotation time, a time required for 360° of probe revolution, for these enzymes (Fig. 3D–F), and rotation rates were calculated from the geometric means of them [21]. The rates for the  $F_0F_1$  with  $\epsilon$ -Cyt and  $\epsilon$ -FlavR were 185 and 148 rps, respectively (Table 2). It was surprising that these rates were similar to that of the wild type (172 rps).

The revolutions of the beads attached to  $F_0F_1$  with  $\epsilon$ -Cyt or  $\epsilon$ -FlavR were reproducibly observed, and their frequencies were essentially the same as those attached to the wild-type enzyme. Degradation of  $\epsilon$ -Cyt or  $\epsilon$ -FlavR in  $F_0F_1$  was not detected even after prolonged incubation (2 h at room temperature) (Fig. S1, and data not shown). Furthermore, by enzyme reconstitution from the isolated subunits [26] and the mutants lacking  $\epsilon$  subunit [23], it was shown that the  $\epsilon$  subunit is essential for binding of the  $F_1$  sector to the  $F_0$ . Thus, it is difficult to assume that we observed rotations of the  $F_0F_1$  from which modified  $\epsilon$  was released.

Crystal structures of the cytochrome  $b_{562}$  and the flavodoxin reductase have been determined, revealing molecular dimensions of  $23 \times 24 \times 48$  Å and  $30 \times 35 \times 55$  Å, respectively [27,28] (Fig. 1C). Although the precise space size between the two stalks connecting  $F_1$  and  $F_0$  has not been defined, we estimated the spherical space with a diameter of about 30 Å from the electron cryo-microscopy of mitochondrial  $F_0F_1$  [10] (Fig. 1B, shown by a red circle). Thus, the cytochrome  $b_{562}$  could barely pass through the space during rotation. However, it should be difficult or impossible for  $\epsilon$ -FlavR to rotate through the space without distorting the stator and the rotor of the enzyme. Despite these structural limitations,  $F_0F_1$  with  $\epsilon$ -Cyt and  $\epsilon$ -FlavR rotated at essentially the same rate as that with the wild-type  $\epsilon$ .

These results suggested that the  $F_0F_1$  had intrinsic elasticity to accommodate flexibility of rotation. The elasticity of the central stalk had been suggested from the measurement of torsional flexibility [29,30]. The elastic rotation was thought to be important for functional coupling between the  $F_0$  and the  $F_1$  [29]. However, the rotations of the  $F_0F_1$  with  $\epsilon$ -Cyt and  $\epsilon$ -FlavR were partially uncoupled to ion pumping, their DCCD sensitivities were substantially

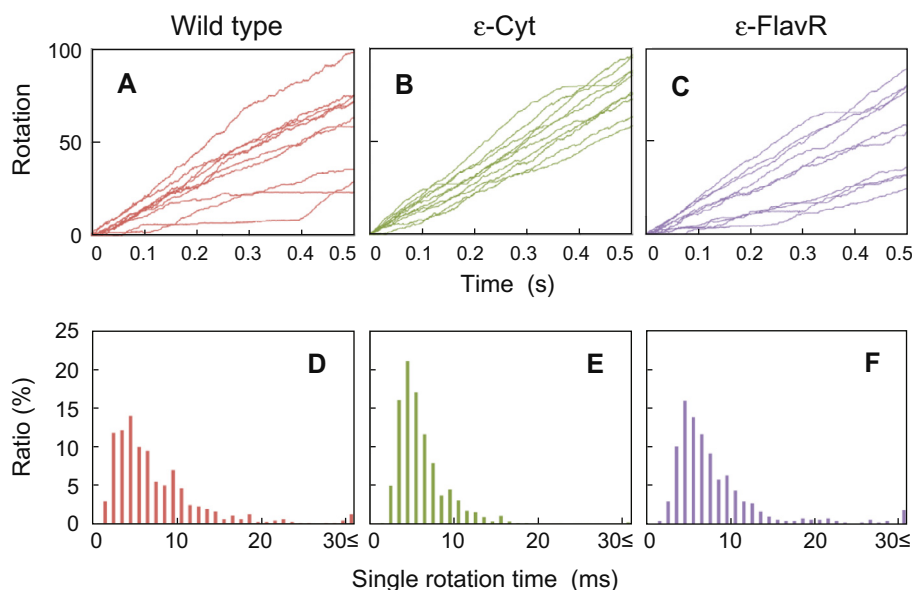


**Fig. 3.** Single molecular rotations of the  $F_0F_1$  with wild-type  $\epsilon$ ,  $\epsilon$ -Cyt and  $\epsilon$ -FlavR. (A–C) Time courses of  $F_0F_1$  with wild-type  $\epsilon$  (A),  $\epsilon$ -Cyt (B) and  $\epsilon$ -FlavR (C) were immobilized and followed rotations as Fig. 1B. Images of the beads were observed by the dark-field microscopy and captured during 0.5 s in 2000 fps (frame rate). Time courses of beads used for calculating rotation rates are shown. (D–F) Single rotation time of  $F_0F_1$  with wild-type  $\epsilon$  (D),  $\epsilon$ -Cyt (E) and  $\epsilon$ -FlavR (F). Histograms of single rotation times required for 360° revolution obtained for ten randomly selected beads attached to the  $F_0F_1$  with wild-type  $\epsilon$  (D),  $\epsilon$ -Cyt (E) and  $\epsilon$ -FlavR (F) [21]. The total rotations analyzed were 598, 798 and 561 for the  $F_0F_1$  with wild-type  $\epsilon$ ,  $\epsilon$ -Cyt and  $\epsilon$ -FlavR, respectively.



reduced (Table S1). We conclude that the intra-molecular rotation of  $F_0F_1$  is elastic but proton transport requires more precise interaction between subunit  $a$  and  $c$ -ring. Thus, large structural perturbation of the central or the peripheral stalk due to passage of the fused protein reduced coupling of rotation to proton transport, as shown for rotation of  $F_0F_1$  with  $\epsilon$ -Cyt and  $\epsilon$ -FlavR.

## Acknowledgments

This study was supported partly by the Japan Society for the Promotion of Science, the Terumo Life Science Foundation, Japan Foundation for Applied Enzymology, and Hayashi Memorial Foundation for Female Natural Scientists (to M.N.-M.). This study was also supported by Grant-in-Aid for Scientific Research from the Ministry of Education, Culture, Sports, Science and Technology, Japan. We are grateful to Ms. Shio Yano for her expert technical assistance.

## Appendix A. Supplementary data

Supplementary data associated with this article can be found, in the online version, at <http://dx.doi.org/10.1016/j.bbrc.2014.03.021>.

## References

- [1] P.D. Boyer, The ATP synthase – a splendid molecular machine, *Annu. Rev. Biochem.* 66 (1997) 717–749.
- [2] M. Futai, G.H. Sun-Wada, Y. Wada, Proton translocating ATPase: including unique enzymes coupling catalysis and proton translocation through mechanical rotation, in: M. Futai, Y. Wada, J. Kaplan (Eds.), *Handbook of ATPases: Biochemistry, Cell Biology, Pathology*, Wiley-VCH Verlag, Weinheim Germany, 2004, pp. 237–260.
- [3] R.K. Nakamoto, J.A. Baylis Scanlon, M.K. Al-Shawi, The rotary mechanism of the ATP synthase, *Arch. Biochem. Biophys.* 476 (2008) 43–50.
- [4] Y. Sambongi, Y. Iko, M. Tanabe, H. Omote, A. Iwamoto-Kihara, I. Ueda, T. Yanagida, Y. Wada, M. Futai, Mechanical rotation of the  $c$  subunit oligomer in ATP synthase ( $F_0F_1$ ): direct observation, *Science* 286 (1999) 1722–1724.
- [5] O. Pänke, K. Gumbiowski, W. Junge, S. Engelbrecht, F-ATPase: specific observation of the rotating  $c$  subunit oligomer of  $EF_0F_1$ , *FEBS Lett.* 472 (2000) 34–38.
- [6] M. Tanabe, K. Nishio, Y. Iko, Y. Sambongi, A. Iwamoto-Kihara, Y. Wada, M. Futai, Rotation of a complex of the  $\gamma$  subunit and  $c$  ring of *Escherichia coli* ATP synthase. The rotor and stator are interchangeable, *J. Biol. Chem.* 276 (2001) 15269–15274.
- [7] K. Nishio, A. Iwamoto-Kihara, A. Yamamoto, Y. Wada, M. Futai, Subunit rotation of ATP synthase embedded in membranes:  $a$  or  $\beta$  subunit rotation relative to the  $c$  subunit ring, *Proc. Natl. Acad. Sci. USA* 99 (2002) 13448–13452.
- [8] M. Diez, B. Zimmermann, M. Börsch, M. König, E. Schweinberger, S. Steigmiller, R. Reuter, S. Felekyan, V. Kudryavtsev, C.A.M. Seidel, P. Gräber, Proton-powered subunit rotation in single membrane-bound  $F_0F_1$ -ATP synthase, *Nat. Struct. Mol. Biol.* 11 (2004) 135–141.
- [9] I.N. Watt, M.G. Montgomery, M.J. Runswick, A.G.W. Leslie, J.E. Walker, Bioenergetic cost of making an adenosine triphosphate molecule in animal mitochondria, *Proc. Natl. Acad. Sci. USA* 107 (2010) 16823–16827.
- [10] L.A. Baker, I.N. Watt, M.J. Runswick, J.E. Walker, J.L. Rubinstein, Arrangement of subunits in intact mammalian mitochondrial ATP synthase determined cryo-EM, *Proc. Natl. Acad. Sci. USA* 109 (2012) 11675–11680.
- [11] S. Wilkens, F.W. Dahlquist, L.P. McIntosh, L.W. Donaldson, R.A. Capaldi, Structural features of the  $\epsilon$  subunit of the *Escherichia coli* ATP synthase determined by NMR spectroscopy, *Nat. Struct. Biol.* 2 (1995) 961–967.
- [12] U. Uhlin, G.B. Cox, J.M. Guss, Crystal structure of the  $\epsilon$  subunit of the proton-translocating ATP synthase from *Escherichia coli*, *Structure* 5 (1997) 1219–1230.
- [13] G. Cingolani, T.M. Duncan, Structure of the ATP synthase catalytic complex ( $F_1$ ) from *Escherichia coli* in an autoinhibited conformation, *Nat. Struct. Mol. Biol.* 18 (2011) 701–707.
- [14] S.D. Dunn, R.G. Tozer, V.D. Zadorozny, Activation of *Escherichia coli*  $F_1$ -ATPase by lauryldimethylamine oxide and ethylene glycol: relationship of ATPase activity to the interaction of the  $\epsilon$  and  $\beta$  subunits, *Biochemistry* 29 (1990) 4335–4340.
- [15] S.P. Tsunoda, A.J. Rodgers, R. Aggeler, M.C. Wilce, M. Yoshida, R.A. Capaldi, Large conformational changes of the  $\epsilon$  subunit in the bacterial  $F_1F_0$  ATP synthase provide a ratchet action to regulate this rotary motor enzyme, *Proc. Natl. Acad. Sci. USA* 98 (2001) 6560–6564.
- [16] V.V. Buligin, T.M. Duncan, R.L. Cross, Rotor/Stator interactions of the  $\epsilon$  subunit in *Escherichia coli* ATP synthase and implications for enzyme regulation, *J. Biol. Chem.* 279 (2001) 35616–35621.
- [17] D.J. Cipriano, Y. Bi, S.D. Dunn, Genetic fusions of globular proteins to the  $\epsilon$  subunit of the *Escherichia coli* ATP synthase: implications for *in vivo* rotational catalysis and  $\epsilon$  subunit function, *J. Biol. Chem.* 277 (2002) 16782–16790.
- [18] M. Nakanishi-Matsui, S. Kashiwagi, H. Hosokawa, D.J. Cipriano, S.D. Dunn, Y. Wada, M. Futai, Stochastic high-speed rotation of *Escherichia coli* ATP synthase  $F_1$  sector: the  $\epsilon$  subunit-sensitive rotation, *J. Biol. Chem.* 281 (2006) 4126–4131.
- [19] H. Hosokawa, M. Nakanishi-Matsui, S. Kashiwagi, I. Fujii-Taira, K. Hayashi, A. Iwamoto-Kihara, Y. Wada, M. Futai, ATP-dependent rotation of mutant ATP synthases defective in proton transport, *J. Biol. Chem.* 280 (2005) 23797–23801.
- [20] A. Iwamoto, H. Omote, H. Hanada, et al., Mutations in Ser174 and the glycine-rich sequence (Gly149, Gly150, and Thr156) in the  $\beta$  subunit of *Escherichia coli*  $H^+$ -ATPase, *J. Biol. Chem.* 266 (1991) 16350–16355.
- [21] M. Nakanishi-Matsui, S. Kashiwagi, T. Ubukata, A. Iwamoto-Kihara, Y. Wada, M. Futai, Rotational catalysis of *Escherichia coli* ATP synthase  $F_1$  sector. Stochastic fluctuation and a key domain of the  $\beta$  subunit, *J. Biol. Chem.* 282 (2007) 20698–20704.
- [22] M. Sekiya, R.K. Nakamoto, M.K. Al-Shawi, M. Nakanishi-Matsui, M. Futai, Temperature dependence of single molecule rotation of the *Escherichia coli* ATP synthase  $F_1$  sector reveals the importance of  $\gamma$ - $\beta$  subunit interactions in the catalytic dwell, *J. Biol. Chem.* 284 (2009) 22401–22410.
- [23] M. Kuki, T. Noumi, M. Maeda, A. Amemura, M. Futai, Functional domains of  $\epsilon$  subunit of *Escherichia coli*  $H^+$ -ATPase ( $F_0F_1$ ), *J. Biol. Chem.* 263 (1988) 17437–17442.
- [24] O.H. Lowry, N.J. Rosebrough, A.L. Farr, R.J. Randall, Protein measurement with the Folin phenol reagent, *J. Biol. Chem.* 193 (1951) 265–275.
- [25] M.M. Bradford, Rapid and sensitive method for the quantitation of microgram quantities of protein utilizing the principle of protein-dye binding, *Anal. Biochem.* 72 (1976) 248–254.
- [26] S.D. Dunn, M. Futai, Reconstitution of a functional coupling factor from the isolated subunits of *Escherichia coli*  $F_1$  ATPase, *J. Biol. Chem.* 255 (1980) 113–118.
- [27] F. Lederer, A. Glatigny, P.H. Bethge, H.D. Bellamy, F.S. Mathews, Improvement of the 2.5 Å resolution model of cytochrome  $b_{562}$  by redetermining the primary structure and using molecular graphics, *J. Mol. Biol.* 148 (1981) 427–448.
- [28] M. Ingelman, V. Bianchi, H. Eklund, The three-dimensional structure of flavodoxin reductase from *Escherichia coli* at 1.7 Å resolution, *J. Mol. Biol.* 26 (1997) 147–157.
- [29] A. Wachter, Y. Bi, S.D. Dunn, B.D. Cain, H. Sielaff, F. Wintermann, S. Engelbrecht, W. Junge, Two rotary motors in F-ATP synthase are elastically coupled by a flexible rotor and a stiff stator stalk, *Proc. Natl. Acad. Sci. USA* 108 (2011) 3924–3929.
- [30] H. Sielaff, H. Rennekamp, A. Wachter, H. Xie, F. Hilders, K. Feldbauer, S.D. Dunn, S. Engelbrecht, W. Junge, Domain compliance and elastic power transmission in rotary  $F_0F_1$ -ATPase, *Proc. Natl. Acad. Sci. USA* 105 (2008) 17760–17765.